Journal of The Electrochemical Society, **156** (5) H372-H377 (2009)
0013-4651/2009/156(5)/H372/6/$23.00 © The Electrochemical Society

Derivation of Rate Constants for the Batch Furnace Radical Oxidation of Silicon Wafers via Hydrogen Combustion

Jeff Bailey,[a,z] Thomas Qiu,[*,b] Hood Chatham,[a] Helmuth Treichel,[c] and Khalid Mohamed[d]

Aviza Technology, Scotts Valley, California, USA 95066

Deal–Grove oxidation rate constants for the controlled combustion-based radical oxidation of silicon wafers in a batch reactor were determined, thus providing insight into the rate-limiting factors. Re-examination of the oxidation rates of wafers with different crystal orientations provides an estimate of the enhancement of the linear rate constant in radical oxidations as compared to standard wet and dry oxidation processes.
© 2009 The Electrochemical Society. [DOI: 10.1149/1.3095468] All rights reserved.

Manuscript submitted May 20, 2008; revised manuscript received January 21, 2009. Published March 25, 2009.

Oxidation of silicon wafers via atomic oxygen radicals is becoming increasingly desirable and has already supplanted conventional wet or dry thermal oxidation for some applications. Growth rates for radical oxidation depend much less on crystal orientation than for thermal dry or wet oxidation, a vital characteristic for three-dimensional transistor designs[1,2] and shallow-trench isolation (STI) liner oxides, for which the lack of sufficient corner rounding from thermal oxidation is a liability.[3] Radical-based oxide films have been shown to have superior breakdown voltages and leakage properties compared to thermal oxides.[4]

At low temperatures, oxide growth rates from oxygen radicals are much higher than thermal oxidation rates. Radicals even enable wafer processing at temperatures below 400°C, a temperature range otherwise only accessible with plasmas. Various methods have long been explored to produce high-quality silicon dioxide at reduced temperatures. Examples include ozone oxidation, UV-assisted oxidation, and plasma oxidation. One single-wafer-based radical oxidation system, known as in situ steam generation (ISSG), utilizes oxygen and hydroxyl radicals created through chemical reactions of hydrogen and oxygen. Its success relies on two critical conditions. First, the process must be run at low pressures to achieve a sufficiently long radical lifetime. Second, a high volume of oxygen and hydrogen must be used to reduce the chemical residence time.[5,6] The reactants are premixed at relatively low temperatures, e.g., 100°C, and flow over a heated silicon wafer. The reactants are heated by the wafer within the thermal boundary layer. Due to the low operating pressure and high mass flow rate, reactants flow over the wafer at high speeds. The silicon wafer has to be heated and maintained at a sufficiently high temperature to initiate and sustain the gas-phase combustion process. This raises the minimum temperature at which combustion-based radical oxidation can be performed, compared to a hotwall reactor, for example.

The challenge for producers of capital equipment for semiconductor manufacturing has been to design radical oxidation systems that are not cost prohibitive, have high throughput, and produce wafers with superior oxide properties (e.g., thickness uniformity). With these targets in mind, it becomes important to understand the nature of the radical-based oxidation, that is, to identify the rate-limiting factors, factors that have been long understood for thermal oxidation. Recently a model for the oxidation kinetics in two combustion-based systems was proposed in which an initial radical-based oxidation regime dominates for thin oxides and is supplanted by wet oxidation for thicker oxides.[7] But what is still lacking is insight into the energetics of the system, activation energies for the oxidation reaction and the oxidant diffusion, that can be used to identify the oxidizing species through phenomena more directly based on the physics and chemistry of silicon oxidation.

Silicon thermal oxidation via reaction with H_2O (wet oxidation) or O_2 (dry oxidation) is typically discussed in context with the Deal–Grove model (DG),[8] which describes diffusion of an oxidant through an overlying oxide to the silicon–oxygen interface where the oxidant reacts with silicon and produces more oxide. The DG model is useful to identify oxidation regimes in which oxidation rate is limited by either the silicon reaction rate or the oxidant diffusion rate through the oxide, corresponding to thin or thick oxides where the growth rates are linear or parabolic, respectively. Comparison of the thermal activation energies for these rate-limiting factors for both wet and dry oxidation also provides insight into the microscopic mechanism responsible.

The DG theory for wet and dry oxidation allows the derivation of a generalized expression for oxide thickness x as a function of time t and three adjustable parameters

$$x^2 + Ax - B(t + \tau) = 0 \qquad [1]$$

where B is known as the parabolic rate constant, B/A as the linear rate constant, and τ is a time displacement to allow for the initial oxide at $t = 0$. For short and long oxidation times Eq. 1 reduces to linear and parabolic growth laws

$$x = \frac{B}{A}(t + \tau) \qquad [2]$$

and

$$x^2 = B(t + \tau) \qquad [3]$$

For purely linear or parabolic growth regimes, the appropriate rate constant can be derived by fitting experimental data to Eq. 2 or 3, often by drawing a line through the points on an (x vs t) or (x^2 vs t) plot. For intermediate times and thicknesses, nonlinear curve-fitting techniques must be used to determine the constants via fitting the data to Eq. 1.

The parabolic rate constant B is related to the diffusivity D of the oxidant in the oxide layer by

$$B = \frac{2DC^*}{N} \qquad [4]$$

where C^* is the peak oxidant concentration in the oxide and N is the number density of oxygen atoms in the silicon dioxide. With fixed oxidant concentration, as in typical wet or dry oxidations, B is proportional to the oxidant diffusivity. Hence, the temperature dependence of B can be used to identify the oxidant, because it should be very close to the known temperature dependence of the diffusivity of the oxidant in SiO_2. For example, the temperature activation energies of the parabolic constants in wet and dry oxidation are 0.71 and 1.24 eV, respectively. These match well to the respective activation energies of diffusion of H_2O and O_2 in SiO_2: 0.80 and 1.17 eV.[9]

* Electrochemical Society Active Member.
[a] Present address: NanoGram Corporation, Milpitas, California 95035, USA.
[b] Present address: SunPower Corporation, San Jose, California 95134, USA.
[c] Present address: Xyratex, Scotts Valley, California 95035, USA.
[d] Present address: PerkinElmer Optoelectronics, Fremont, California 94538, USA.
[z] E-mail: jbailey@nanogram.com

The linear rate coefficient B/A is independent of diffusivity but related to the reaction rate of the oxidant at the silicon–oxide interface. The thermal activation energies for both wet and dry thermal oxidation are close to 2.0 eV, suggesting a similar rate-limiting factor in both cases. The thermal activation energy is believed to be associated with the energy required to break silicon–silicon bonds.

An understanding of growth rates, oxidation regimes, and activation energies for radical-based oxidation would help in understanding the atomic nature of the process. Detailed analysis of the rate constants could help identify whether different rate-limiting factors exist for radical oxidation.

From a practical point of view, one needs to understand when radical oxidation occurs vs conventional thermal oxidation. In a combustion-based oxidation system, in which oxygen radicals are short-lived intermediate species in the reaction of H_2 with O_2, both a reactant (O_2) and the product (H_2O) are oxidizers of silicon. For this application it is essential to distinguish the mode of oxidation, that is, whether oxidation occurred via radicals or via thermal oxidizers. Identification of radical oxidation rate constants defined in the DG model would allow making this distinction.

This paper describes the results of a series of oxidations of silicon wafers using a batch-type combustion-based radical oxidation system, characterization and measurement of the oxide films, and an analysis of the oxidation rates. The results are compared to typical results expected for wet or dry oxidations under similar conditions.

Experimental

Silicon wafers (300 mm diameter, ⟨100⟩ orientation, prime wafers with no pretreatment) were processed in a 100-wafer vertical batch reactor produced by Aviza Technology.[10] This reactor is of the "across-flow" style, in which a vertical gas injector distributes the inlet gases evenly among all 100 wafers in the load. The system differs from the ISSG apparatus in that both hydrogen and oxygen are preheated to a process temperature separately before being introduced into the batch reaction chamber. The gases react in the wafer vicinity, and the products are removed via a distributed exhaust plenum. The hotwall reactor is designed so that the gases flow in a horizontal direction and all wafers have essentially the same processing environment, thereby yielding highly uniform on-wafer results. Because the reactor does not require the wafers to heat the reactants, radical oxidation can be achieved at lower temperatures than with single-wafer systems like ISSG.

Because a principal purpose of the experiments is to estimate the activation energies of the radical oxidation rate constants, all process conditions were fixed except the temperature. Radicals were generated by the combustion of H_2 in O_2, for which the H_2:O_2 flow ratio was 1:1. The pressure was held constant at 500 mTorr. The wafer boat was fully loaded with wafers at the onset of the oxidation, and the process was stopped and three sample wafers removed after 2, 8, 32, 120, and 480 min of total oxidation time to develop a time series of oxide layer thickness. (Oxidation was halted by first turning off the oxygen flow to prevent dry oxidation during wafer removal.) This entire procedure was repeated for otherwise identical conditions at 600, 700, 800, and 900°C. Oxide thickness maps were obtained for each set of three wafers using a Nanometrics NanoSpec 3000. Forty-nine points were measured per wafer, and the average

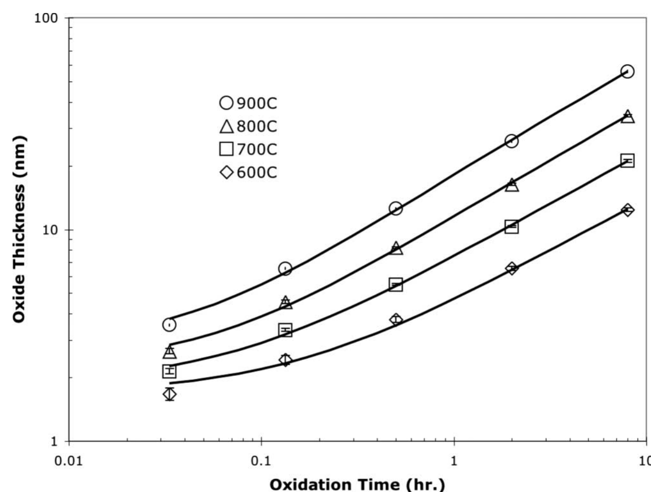

Figure 1. Oxide thickness vs time with least-squares fits to Eq. 1 (700–900°C) and Eq. 3 (600°C). Each plotted point and error bar are the average and standard deviation, respectively, of oxide thicknesses measured on three sample wafers at 49 points per wafer.

thickness and standard deviation among each three-wafer set were used as a single data point for each combination of time and temperature in the subsequent analysis.

Results and Discussion

Without any prior knowledge of the growth regime in our experiments, it was necessary to use a nonlinear least-squares (Marquardt–Levenberg[11]) curve-fitting algorithm to estimate the DG rate constants. The time series data are plotted in Fig. 1, fit to Eq. 1 with the fit parameters indicated. For the 600°C data an acceptable fit to Eq. 1 was not possible, so the data were fit to Eq. 3 instead, yielding information only on the parabolic constant at that temperature. Because the native thermal oxide was of no certain origin or composition and was not the result of radical oxidation, the native oxide thickness was not included in the curve fits. The changing nature of the oxide may have introduced some error into the curve fits, especially for the thinnest values. The DG fit parameters and their uncertainties are listed in Table I.

As mentioned previously, for wet or dry oxidation the temperature dependence of the parabolic rate constant directly yields information about the oxidant diffusivity. In our case, however, because the oxygen radicals themselves are generated in a spontaneous chemical reaction, it is not appropriate to use the same analysis without consideration of the radical concentration C^*. Deriving the activation energy of the parabolic constant alone fails to take into account the temperature dependence of the radical oxygen concentration. Therefore, estimates of the radical oxygen concentration were made by numerical simulations of the combustion reaction. A 22-step gas-phase reaction mechanism derived from the H–O subset of a hydrocarbon combustion mechanism[12] was used with CHEMKIN software,[13] employing the perfectly stirred reactor module with actual process conditions and appropriate approximations

Table I. Nonlinear least-squares fit parameters of the data in Fig. 1 to Eq. 1 (700–900°) and Eq. 3 (600°C) with their estimated uncertainties.

Temperature (°C)	A (nm)	ΔA (nm)	B (nm^2/h)	ΔB (nm^2/h)	τ (h)	$\Delta\tau$ (h)
600	n/a	n/a	19.2	0.587	0.150	0.031
700	0.650	1.02	56.3	2.97	0.084	0.046
800	3.66	1.59	162	7.72	0.081	0.034
900	7.72	2.05	438	16.4	0.066	0.023

Table II. Calculated species volume fractions for the oxidation conditions used in the time series.

Temperature (°C)	Pressure (Torr)	Volume fractions							
		H_2O	O_2	H	O	H_2	OH	HO_2	H_2O_2
600	0.5	0.367	0.336	0.205	0.0262	0.0619	0.0040	8.19×10^{-7}	1.32×10^{-8}
700	0.5	0.367	0.321	0.215	0.0414	0.0485	0.0068	5.78×10^{-7}	1.93×10^{-8}
800	0.5	0.363	0.310	0.213	0.0558	0.0462	0.0107	4.24×10^{-7}	2.70×10^{-8}
900	0.5	0.360	0.302	0.207	0.0685	0.0477	0.0158	3.22×10^{-7}	3.58×10^{-8}

of the reactor geometry. Calculated oxygen radical concentrations depend upon assumptions of the likelihood of radical recombination at surfaces. Previous simulations of these reactions by the authors have been successful using an estimated reactive sticking coefficient of 1×10^{-4} for atomic oxygen. Steady-state values of the species volume fractions at the wafer surfaces were calculated and are shown in Table II. (This is a reasonable approach, especially because the temperature dependence is more important than the actual values at any temperature, and temperature-dependent gas-phase reaction rates are well known.) The unmodified B values were divided by the radical fractions to produce corrected values B^*. Arrhenius plots of the raw (not adjusted) and corrected (adjusted for radical concentration) coefficients are shown in Fig. 2, including a weighted linear least-squares fit to the data points.

Because information on the linear rate coefficient B/A was available for all but one temperature, a similar analysis was performed for the linear coefficient. Although the linear constant is independent of diffusivity, it is still proportional to oxidant concentration. A similar modification of the linear rate constants had to be performed; Arrhenius plots for the nonadjusted and adjusted linear rate coefficients are shown in Fig. 3.

From the linear least-squares fits to the points plotted in Fig. 2 and 3, the expressions for the modified parabolic (B^*) and linear $[(B/A)^*]$ rate constants are

$$\ln B^* = 14.8(0.6) - \frac{7250(590)}{T} \quad [5]$$

$$\ln\left(\frac{B}{A}\right)^* = 5.5(2.8) \quad [6]$$

appropriate for radical oxidation at 500 mTorr total pressure. Uncertainties in the values are in parentheses. The actual rate constants B and B/A are obtained by multiplying the modified constants by the volume fraction of atomic oxygen at the wafer surface. Equation 6 lacks any temperature dependence, consistent with Fig. 3.

Discussion

Without prior assumptions that the DG analysis would yield useful results, we found good agreement with our experimental data and DG theory. Although the measured thicknesses matched well with the generalized rate Eq. 1, the thicknesses measured after 2 min of oxidation are all slightly lower than predicted by the best-fit DG rate expression. This may be due to effects related to the native oxide, or instead to transient effects associated with starting and stopping the oxidant gas in a batch furnace. Shorter oxidation times might provide more insight, but due to the size of the reactor, oxidation times shorter than 2 min are not practical. Given the consistency of all the results, we believe the estimated linear rate constant values (and their calculated uncertainties) are reliable.

The standard DG rate equations assume no loss of oxidant due to recombination or parasitic reactions in the oxide. Recombination might be expected with radical oxygen as the diffusing and oxidizing species, for example. Under the conditions used in the experiments described here, however, we feel recombination or loss of oxidant is unimportant for two reasons. First, the oxides formed in these experiments are very thin, only a few nanometers in most cases. Second, the recombination rate of atomic oxygen into diatomic oxygen is expected to be second-order in the atomic oxygen concentration ($O + O \rightarrow O_2$), and at the low pressures and radical fractions for these process conditions we expect radical recombination to be very unlikely. Moreover, we found good agreement between predicted and measured oxide thicknesses over a large range in pressures, as shown below.

Analysis of the temperature dependence of the parabolic rate constant suggests the oxidant in these experiments diffuses through

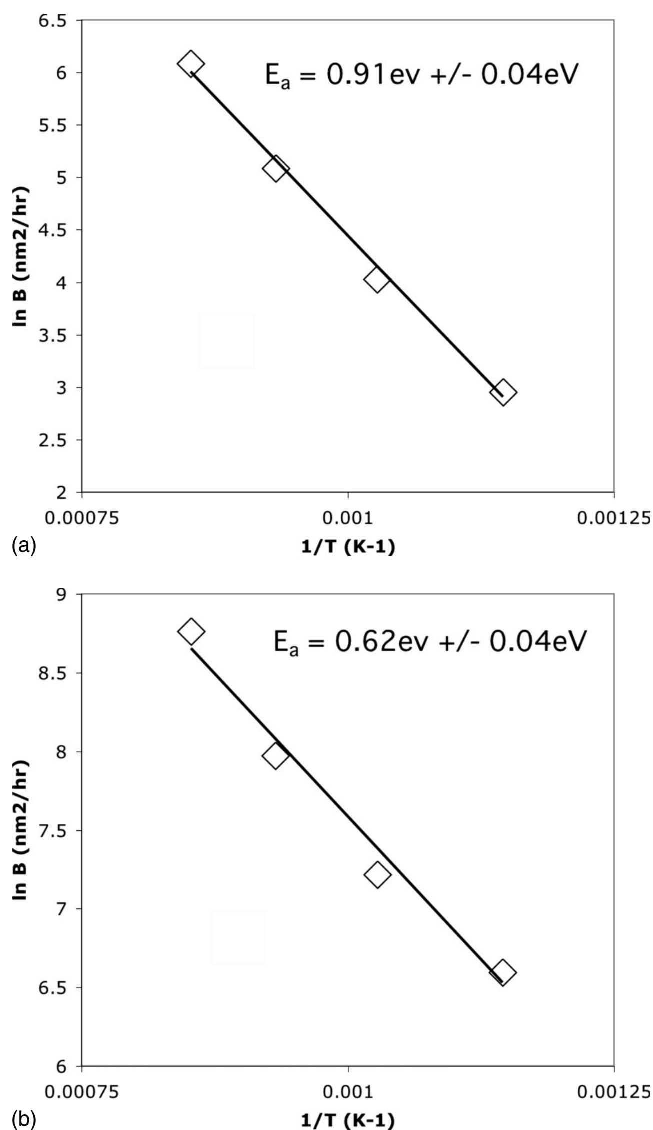

Figure 2. Parabolic rate coefficients vs inverse temperature: (a) unadjusted for oxygen radical concentration and (b) adjusted for oxygen radical concentration.

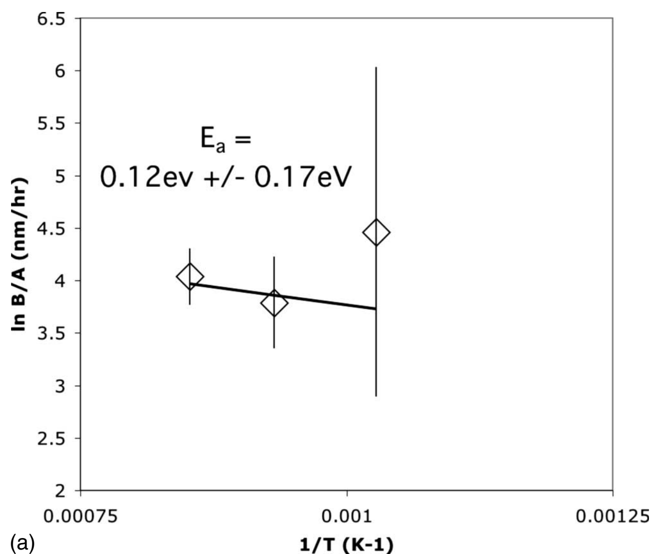

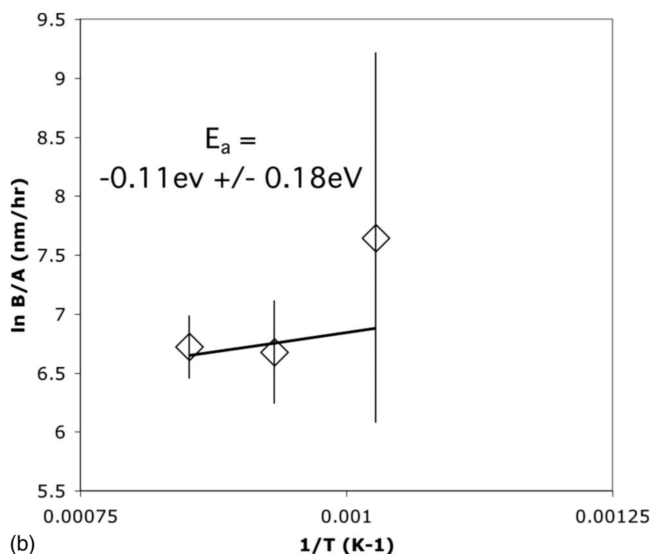

Figure 3. Linear rate coefficients vs inverse temperature: (a) unadjusted for oxygen radical concentration and (b) adjusted for oxygen radical concentration.

the silicon dioxide with thermal activation energy close to 0.63 eV. This value is significantly less than that for H_2O (0.80 eV) and very much less than that for O_2 (1.17 eV). The parabolic rate constant alone is a strong indicator for a radical species with high diffusivity, consistent with atomic oxygen as the oxidant. The activation energy of the radical oxidation linear rate coefficient reported here is essentially zero and therefore differs strikingly from that for thermal oxidation. This indicates that the oxidant is a highly excited species, consistent with the conclusion that oxygen radicals, with a standard state enthalpy near 2.6 eV, are the oxidizing species. Oxygen radicals provide more than enough energy to break the silicon–silicon bond, and measured activation energy of zero for the linear rate constant is therefore expected.

Both the linear and parabolic rate constants obtained here rule out the possibility that molecular oxygen is the primary oxidant. The parabolic rate constant results allow the possibility that another fast diffuser, e.g., hydroxyl groups with diffusivity in amorphous silica near 0.5 eV,[14] are the oxidant. But even if one assumes that hydroxyl groups are the diffusing species, the exceedingly high growth rate at low temperatures rules out the possibility that this is wet oxidation. The estimation of the thermal activation energy of the

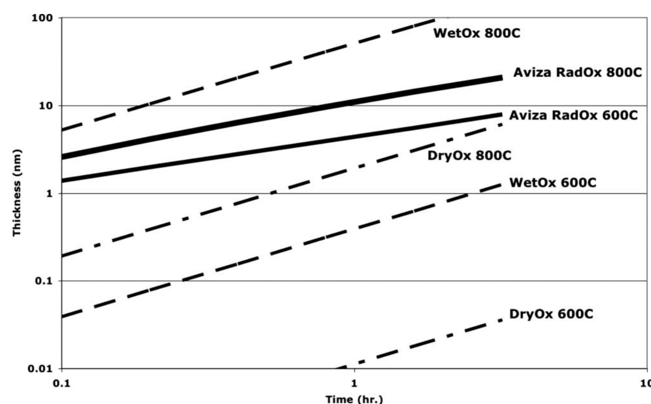

Figure 4. Predicted oxide thicknesses for atmospheric-pressure wet and dry oxidation and low-pressure combustion-based radical oxidation described in this paper.

linear rate coefficient allows us to state with certainty that an excited species with high diffusivity, most likely atomic oxygen, is the oxidizing species.

This is an even more obvious conclusion when the predicted oxide thicknesses for atmospheric-pressure thermal oxidations are compared against thicknesses for 500 mTorr combustion-based radical oxidation, depicted in Fig. 4. Extrapolation of the radical oxidation curves suggests that 600°C is not the lower limit for the combustion-based radical oxidation. In fact, uniform oxide layers have been grown on wafers at temperatures even below 400°C using the combustion-based radical oxidation process at Aviza Technology.

The utility of the derivation of the DG rate constants can be demonstrated in a re-evaluation of previously published data. The benefit of the relative insensitivity of oxide thickness to crystal orientation is shown in a pair of transmission electron microscopy (TEM) images of shallow trench structures processed in radical or thermal oxidations (Fig. 5). The liner thickness variation is much smaller along the trench sidewalls, corners, and bottom with the radical oxide. This result was also demonstrated in a series of experiments depicted in Fig. 4 in Ref. 10 in which wafers of orientation ⟨100⟩, ⟨110⟩, and ⟨111⟩ were radical-oxidized for 30 min at temperatures from 700 to 900°C and pressures from 1 to 4.6 Torr. Given the rate constants presented above (with oxidant concentration adjusted for pressure) and the results of combustion chemistry simulations described above, it is possible to predict the oxide thicknesses (on ⟨100⟩ wafers) for these conditions. Table III summarizes the pressure, temperature, and the calculated atomic oxygen volume fraction. The measured and predicted oxide thicknesses are in good agreement (see Fig. 6).

Furthermore, it is possible to derive information about the differences in linear rate constants among the wafer orientations based upon the measured thicknesses, the rate constants derived above, and the DG theory. Because the parabolic rate constant is related to the diffusivity of the oxidant through the amorphous oxide layer, it is found to be relatively independent of crystal orientation.[15] The orientation dependence of thermal oxidation is found primarily in the linear rate constant. Assuming that the same is true for radical oxidation and that a difference in measured oxide thickness is due only to a change in the linear rate constant, it is possible to express the fractional change in linear rate constant (B/A) that would produce a specified fractional change in oxide thickness by differentiation of Eq. 1

$$\frac{\Delta(B/A)}{(B/A)} = \left[1 + 2x\frac{(B/A)}{B}\right]\frac{\Delta x}{x} \qquad [7]$$

which has the proper behavior in the limiting cases of very thin and very thick oxides. Although the fractional increase in thickness for

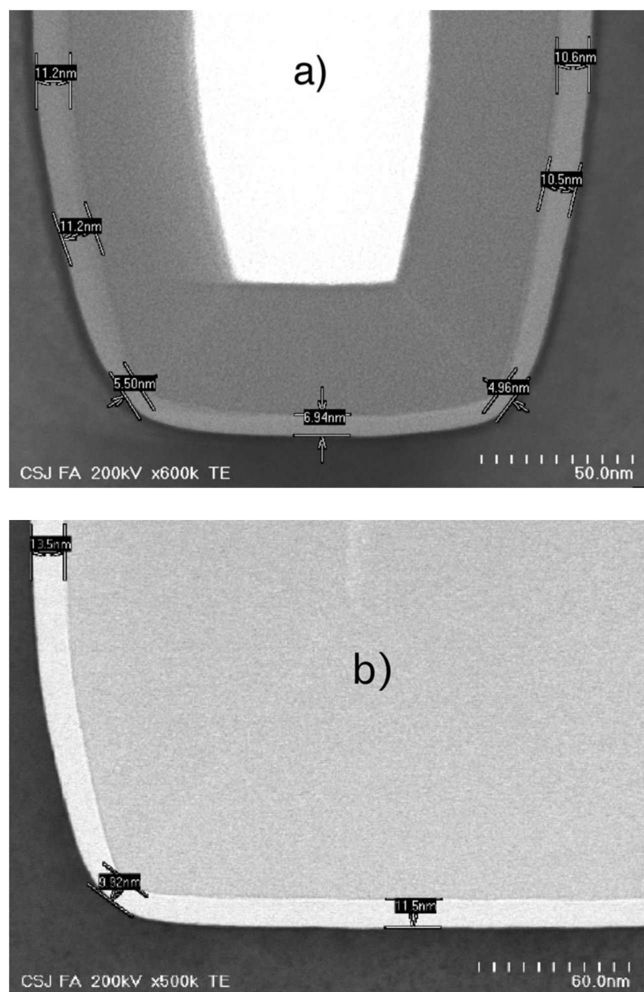

Figure 5. (a) TEM image of STI liner from a 1000°C dry oxidation. Liner thickness ranges from 4.96 to 11.2 nm. (b) TEM image of equivalent liner formed via combustion-based radical oxidation at 700°C. Thickness ranges from 9.9 to 13.5 nm.

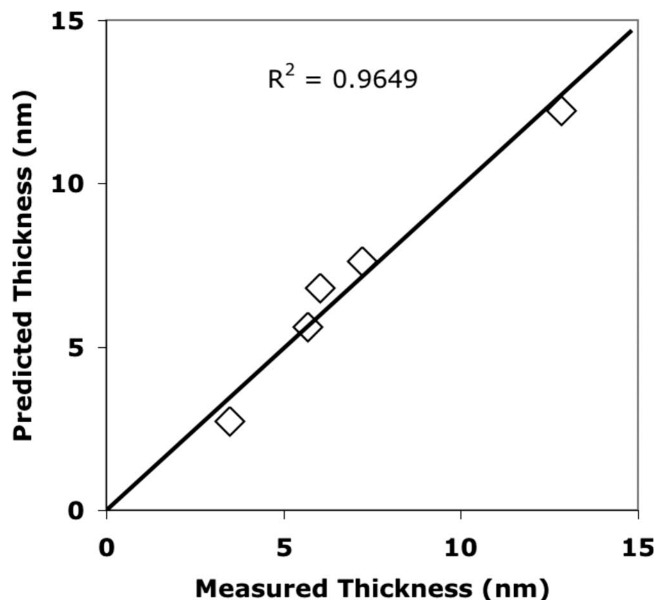

Figure 6. Measured ⟨100⟩ oxide thicknesses (after Fig. 4 of Ref. 11) and predicted values based on estimated rate parameters from this study and calculated atomic oxygen concentrations for each condition. (Assumes an initial time displacement τ of 0.1 h, typical for the time series results.)

⟨110⟩ and ⟨111⟩ orientations averages about 12% among the wafers from Ref. 10, the use of Eq. 7 allows us to determine what increase in the linear rate constant alone would account for the increased thickness. The result turns out to be about a 24% increase in the linear rate constant for both ⟨110⟩ and ⟨111⟩ orientations. This is well below the 68% enhancement for ⟨111⟩ wafers in thermal oxidation, another indication of the different nature of the radical oxidation process. So although this analysis is no substitute for direct time-series measurements on the other wafer orientations, it demonstrates the utility of the estimated rate parameters to derive information consistent with experimental observation.

Table III. Process conditions and calculated atomic O volume fractions for the oxidation conditions described in Ref. 11.

Temperature (°C)	Pressure (Torr)	Atomic O vol. Fraction
800	2.8	0.0127
900	4.6	0.00756
700	4.6	0.00291
700	1	0.0360
900	1	0.0642

The determination of DG rate constants for radical wafer oxidation via hydrogen combustion enables prediction of oxide thicknesses for a wide variety of oxidation conditions, especially when coupled with the predictive capability of combustion reaction simulations.

Conclusions

DG oxidation rate constants for the controlled combustion-based radical oxidation of silicon wafers in a batch reactor were determined. We found good agreement with our experimental data and the standard rate laws. Analysis of the temperature dependence of the parabolic rate constant suggests the oxidant in these experiments diffuses through the silicon dioxide with thermal activation energy close to 0.63 eV. This value is significantly less than that for H_2O (0.80 eV) and very much less than that for O_2 (1.17 eV). The parabolic rate constant alone is a strong indicator for a radical species with high diffusivity, consistent with atomic oxygen with a standard state enthalpy near 2.6 eV as the oxidant. A 24% increase in the linear rate constant for both ⟨110⟩ and ⟨111⟩ orientations is well below the 68% enhancement, e.g., for ⟨111⟩ wafers in thermal oxidations, consistent with experimental observations.

Aviza Technology assisted in meeting the publication costs of this article.

References

1. K. Kim and G. H. Koh, in *The 24th International Conference on Microelectronics*, IEEE, Vol. 1, pp. 377–384 (2004).
2. S. E. Thompson, R. S. Chau, T. Ghani, K. Mistry, S. Tyagi, and M. T. Bohr, *IEEE Trans. Semicond. Manuf.*, **18**, 26 (2005).
3. H. J. L. Forstner, F. Nouri, and C. Olsen, in *Advanced Thermal Processing of Semiconductors, RTP 2003*, IEEE, pp. 163–166 (2003).
4. J. J. Han, K. S. Lee, J. G. Jee, W. Lee, Y. W. Hyung, and H. D. Lee, *J. Korean Phys. Soc.*, **49**, 2028 (2006).
5. R. J. Kee, W. H. Yang, L. L. Raja, and C. A. Wolden, *Proc. Combust. Inst.*, **28**, 1381 (2000).
6. R. J. Kee, W. Yang, N. Sullivan, A. M. Dean, A. Zojaji, M. Hall, and M. Williams, *Proc. Combust. Inst.*, **29**, 1055 (2002).
7. O. Storbeck, W. Pethe, and R. Hayn, *Mater. Sci. Forum*, **573–574**, 147 (2008).
8. J. D. Plummer, M. D. Deal, and P. B. Griffin, *Silicon VLSI Technology–Fundamentals, Practice and Modeling*, Prentice Hall, Englewood Cliffs, NJ (2000).

9. B. E. Deal and A. S. Grove, *J. Appl. Phys.*, **36**, 3770 (1965).
10. T. Qiu, C. Porter, M. Mogaard, J. Bailey, and H. Chatham, *Solid State Technol.*, **2006**, 39.
11. D. W. Marquardt, *J. Soc. Ind. Appl. Math.*, **11**, 431 (1963).
12. http://maeweb.ucsd.edu/~combustion/cermech/
13. R. J. Kee, F. M. Rupley, J. A. Miller, M. E. Coltrin, J. F. Grcar, E. Meeks, H. K. Moffat, A. E. Lutz, G. Dixon-Lewis, M. D. Smooke, et al., CHEMKIN Release 4.1.1, Reaction Design, San Diego, CA (2005).
14. S. Wolf and R. N. Tauber, *Silicon Processing for the VLSI Era, Process Technology*, Vol. 1, p. 262, Lattice Press, Sunset Beach, CA (1986).
15. S. Wolf and R. N. Tauber, *Silicon Processing for the VLSI Era, Process Technology*, Vol. 1, p. 211, Lattice Press, Sunset Beach, CA (1986).